COMMUNICATION

Synthesis of Multifunctional Micrometer-Sized Particles with Magnetic, Amphiphilic, and Anisotropic Properties

*Siyoung Q. Choi, Se Gyu Jang, Andrew J. Pascall, Michael D. Dimitriou, Taegon Kang, Craig J. Hawker, and Todd M. Squires**

Well-defined, functional colloids provide critical model systems for a variety of fundamental phenomena in materials and soft matter, and enable a broad range of technological applications from optics[1] to biotechnology.[2] The ability to fabricate large quantities of colloids with high uniformity and specified shape and function has thus been greatly desired. For example, magnetic colloids can be externally manipulated and controlled, and have been used in applications ranging from photonic crystals,[3] cell sorting,[2] biosensors,[4] drug delivery,[5] biomedical applications,[6] and single-molecule biophysics.[7] Magnetic colloids that can be remotely controlled by applied fields have also been exploited in m-ink,[8] microrheological probes,[9–11] and a variety of self-organizing systems.[12,13] In a similar fashion, ferrofluids and magneto-rheological fluids are frequently used to make useful materials because of their tuneable dynamic response.[14,15]

Another important direction for designing colloids involves shape anisotropy. Anisotropic particles offer additional control of light propagation for photonic crystals[3] and resistance against efficient phagocytosis in drug delivery applications.[16] They can also give rise to interesting and unique behaviors that are not found with spherical particles,[17–24] with examples including self-assembly at fluid/fluid interfaces,[17,18] novel interactions when dispersed in nematic liquid crystals,[19] and non-Newtonian rheological properties.[20,23]

Finally, introducing chemical anisotropy on different faces (so-called "Janus" particles) provides both technological importance and scientific interest.[25–30] For example, such particles can be used for drug delivery, where one side is designed to bind specifically to a cell surface, while the other side incorporates a second functionality that binds a particular drug.[31] Despite the importance of all these functionalities, to our knowledge particles have yet to be synthesized addressing all three structural features: magnetic, anisotropic and Janus functionality.

Here, we present versatile methods to fabricate Janus microparticles of defined, variable shape that exhibit either ferromagnetic or paramagnetic properties. We highlight two examples where such particles open new capabilities in areas of growing interest: the rheology of complex fluid interfaces, and the reversible directed assembly of particles at interfaces. In particular, we have developed a technique in which ferromagnetic Janus microdisks serve as sensitive probes for the active, interfacial microrheology of complex fluid/fluid interfaces. Motivated by recent interest in interfacially-active particles as surfactants, we show triangular paramagnetic microparticles to function as designer building blocks at fluid interfaces: they are stable against capillary aggregation, yet self-assemble under applied magnetic fields.

Surface-active molecules and particles are known to modify the surface energy of fluid interfaces; additionally, they can affect the dynamic behavior of such interfaces materials by imparting a viscosity (or viscoelasticity) to the interface itself. We have recently developed a powerful new technique to measure the rheological properties of complex fluid interfaces.[32] Our technique requires probes with all three functionalities: ferromagnetism, amphiphilicity, and two-dimensional shape anisotropy. In particular, the microprobes must 1) be small, yet visible under optical microscopy (1 to 100 μm); 2) ferromagnetic, so as to enable external forces or torques to be applied; 3) amphiphilic, to ensure the probes physically absorb onto fluid/fluid interfaces; 4) anisotropic, to enable the orientation of a rotating probe to be tracked optically. To meet these demands, we fabricated ferromagnetic, Janus microdisks with two 'buttonholes,' as described below.

A planar (2D) fabrication strategy, enabled by photolithography, is ideally suited for these structural demands, as it allows essentially any planar shape to be designed with various functionalities incorporated through layer-by-layer deposition. While this work builds on recent reports of micrometer-sized particles fabricated by photolithography,[33–35] the introduction of magnetic properties and chemical anisotropy imparts significantly greater utility for the widespread use of these microparticles in a variety of fields.

The schematic photolithographic process for production of these multifunctional microparticles is shown in **Figure 1**. Initially, a 200 nm sacrificial layer (Omnicoat, Microchem) is spin-coated on a 4'' silicon wafer, followed by a one-micrometer layer of photoresist (SU-8, Microchem). The bilayer structure is then

Prof. T. M. Squires
Department of Chemical Engineering
University of California
Santa Barbara, CA 93106, USA
E-mail: squires@engineering.ucsb.edu
S. Q. Choi, A. J. Pascall, Prof. T. M. Squires
Department of Chemical Engineering
University of California
Santa Barbara, CA 93106, USA
S. Q. Choi, Dr. S. G. Jang, Prof. C. J. Hawker, Prof. T. M. Squires
Materials Research Laboratory
University of California
Santa Barbara, CA 93106, USA
M. D. Dimitriou, T. Kang, Prof. C. J. Hawker
Materials Department
University of California
Santa Barbara, CA 93106, USA

DOI: 10.1002/adma.201003604

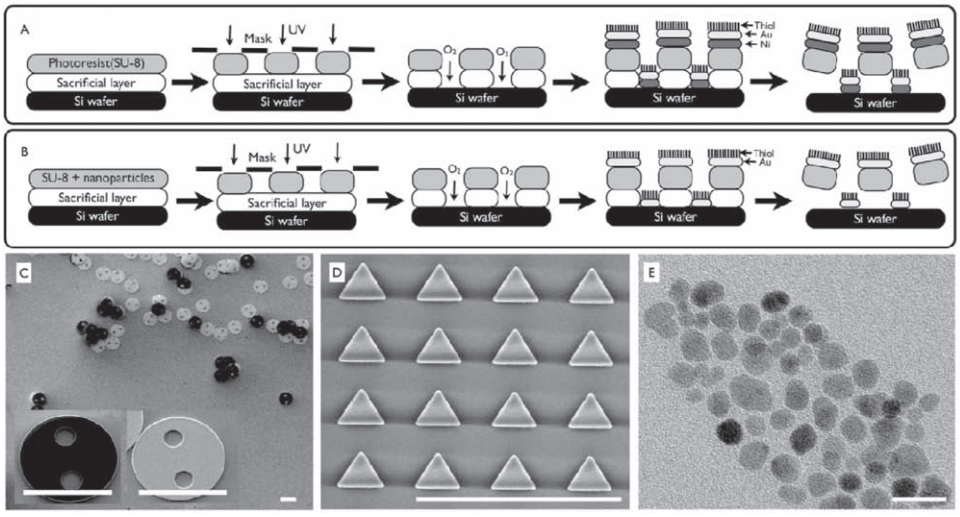

Figure 1. A) Photolithographic process for the microfabrication of ferromagnetic particles. SU-8 particles are initially made photolithographically atop a sacrificial layer. An O_2 plasma etch removes the bare sacrificial layer between the particles. A ferromagnetic nickel layer is evaporatively deposited on SU-8 particles, followed by a gold layer, and the entire wafer is immediately dunked into a solution of thiol-terminated molecules to form a self-assembled monolayer. Chemical etching and sonication removes the sacrificial layer, releasing the particles but not the metal between the particles. B) Paramagnetic particles are microfabricated by dispersing $CoFe_2O_4$ superparamagnetic nanoparticles in SU-8, followed by the same photolithographic process. SEM images of C) 20 μm-diameter ferromagnetic microdisks with two buttonholes, showing different surface functionalities on each side (scale bars: 20 μm), and D) Paramagnetic 4 μm-side triangles (scale bar: 20 μm). E) TEM image of $CoFe_2O_4$ superparamagnetic nanoparticles (scale bar: 20 nm).

baked at 95 °C for 1 min, and photoresist exposed to UV light through a patterned chrome photomask for 3 sec. After developing the photoresist, the wafer is exposed to an oxygen plasma at 0.19 Torr for 2 min, which removes the exposed sacrificial layer but not the sacrificial layer buried under the photoresist structures. (This etch step is critical, as it ensures that the metal layers that are subsequently deposited will remain on the wafer, even while the desired multilayer microparticles are lifted off. By preventing the microparticles from aggregating with magnetic metal fragments, it eliminates the need for an additional process to separate the microparticles from the magnetic metal fragments.) Ferromagnetic functionality is then imparted to the microstructures by depositing a magnetic layer, typically nickel, cobalt or iron (10–300 nm), using electron beam deposition. A 10 nm gold layer is then directly deposited on the magnetic layer which gives rise to a Janus character and allows for facile functionalization with self-assembled monolayers (SAMs) of a wide variety of thiol-terminated molecules. Immediately following Au deposition, the wafers were submerged in a 1 mM solution of 1H,1H,2H,2H-perfluorooctanethiol (Sigma) in ethanol for 8 hours. We then release the microdisks from the wafer by gently sonicating in deionized water. The magnetic character of the microparticles greatly facilitates subsequent purification and collection. XPS analysis (Supporting Information, Figure S1) demonstrates the existence of each of these layers.

To measure the rheology of complex fluid interfaces, we position the ferromagnetic disks on the liquid interface to be probed, then spread the surface-active species on the interface around the probe, and use electromagnets to exert a known, programmable torque on the probe. To do so, the microdisk particles are gently sonicated to uniformly disperse and break up weakly-flocculated microdisk clusters. A few drops of the microdisk solution are then placed on the interface by micropipette, followed by spreading the surfactant of interest. **Figure 2** highlights one example: a ferromagnetic, Janus microbutton probe is made to rotate in an oscillatory fashion within a monolayer of polystyrene colloids. Both the microbutton probe and the colloids are adsorbed at the planar interface between clean, immiscible solvents (pure water and decane). Colloids within the monolayer experience a long-range electrostatic repulsion mediated through the decane,[36] which gives rise to hexagonal crystalline order within the monolayer. Figure 2B shows the frequency-dependent surface visco-elastic shear moduli of the colloidal monolayer itself – a low-frequency elastic plateau is observed, along with increasing visco-elasticity at frequencies above the diffusive relaxation time of colloids within their well. Additionally, Figure 2C shows the weakening – and eventual yielding – of the colloidal monolayer for increasing applied strain, which can be directly correlated with the onset of lattice hopping by particles. (See the movie in the Supporting Information for an example.)

To study the magnetic properties of our structures more quantitatively, a wafer of fabricated microdisks was diced after metal deposition into 3 mm by 3 mm sections, each of which contains approximately 10^4 ferromagnetic microdisks. The *in-plane* magnetic properties of microdisks were then measured using a SQUID (MPMS 5XL, Quantum design) with **Figure 3**A showing the ferromagnetic properties of a representative batch of 20 μm-diameter microdisks incorporating a 150 nm ferromagnetic layer of nickel. It should be noted that the ferromagnetic properties of the microparticles are retained, with hysteresis and saturation of magnetization being observed.

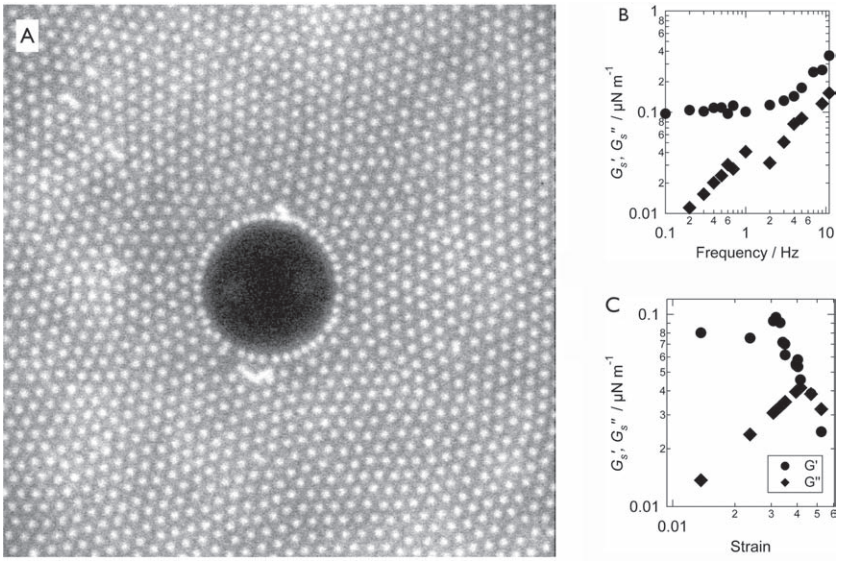

Figure 2. Ferromagnetic microbuttons as probes of the rheology of complex fluid interfaces. A) A Janus, ferromagnetic microbutton (10 μm radius, described in text) is placed at the interface between pure water and decane. A monolayer of 1 μm-diameter polystyrene particles is then spread at the water-decane interface, and mutual electrostatic repulsion between colloids imparts local crystalline order. The visco-elastic moduli of the colloidal monolayer can be determined from the microbutton's rotation in response to an externally imposed oscillatory torque (B-C), (see Supporting Information video). B) The linear viscoelastic modulus of the colloidal monolayer is primarily elastic, with a low frequency plateau. C) Increasing the amplitude of the oscillatory strain reveals a linear elastic response at low strains, with softening and yielding of the monolayer above a critical strain, which direct visualization reveals to correspond to particle hopping between lattice sites (see Supporting Information video).

The microrheological application described above requires a fixed permanent magnetic moment that does not reorient under externally applied fields. The coercivity represents the magnetic field required to demagnetize materials via reorientation of the magnetic moments of the domains. In general, bulk nickel has extremely low coercivity (~1 Oe).[37] The large internal stresses generated during evaporative deposition of Ni films, however, increase coercivity by up to two orders of magnitude (Figure 3B).[37]

Furthermore, we study how the *in-plane* saturation magnetization of our thin Ni films changes with thickness. Unlike bulk materials, whose saturation magnetization (M_s) depends linearly on their volume, the saturation magnetization of thin films shows different behavior (Figure 3C). To compare thin film measurements with predictions based on bulk properties, we estimate M_s based on the volume of the thin film (Figure 3C), orange line). The saturation magnetization M_s of sufficiently thin Nickel films is higher than one would expect based on bulk properties, since magnetic domains prefer their moments to be oriented in the plane of the thin film, rather than randomly as in bulk. However, out-of-plane magnetic moments of the domains become favorable as the film thickness increases to minimize the magnetostatic energy, thus giving rise to smaller *in-plane* magnetization than bulk.

The behavior of particles at interfaces–as surfactants,[38] in stabilizing unusual fluid structures,[39,40] or in forming novel interfacial phases[41] has found increasing interest in recent years. The ability to reversibly induce aggregation and direct self-assembly at fluid interfaces could enable a "tunable" rheology of interfacial phases, much like occurs in three-dimensional ferrofluids or magnetorheological fluids.[15,42,43] The ferromagnetic moments that were crucial for our microrheological probes, however, would lead to irreversible aggregation for interfacial dispersions. Paramagnetic particles are thus better-suited for applications involving suspensions, since they are magnetized only under an ambient field.

One way to synthesize paramagnetic particles involves modifying the deposition procedure. Depositing magnetic metals on non-wetting surfaces generates superparamagnetic "nanodrops".[44] For example, permalloy evaporated onto an organic SAM on gold has been shown to give rise to superparamagnetic properties. However, the magnetic response is rather modest, since only a single layer of the nanodrops forms on the surface. Multiple layers, in principle, could be made through repeated metal depositions and SAM treatments, but such an approach would be impractically time-consuming and expensive.

A more practical, alternative route to anisotropic, Janus colloids with strong superparamagnetic response involves encapsulating superparamagnetic nanoparticles (SPNPs) in a cross-linked polymer matrix.[45] Following this strategy, SPNPs were dispersed in the photoresist (SU-8) and the photolithographic patterning procedure described above followed. An added advantage of this new strategy is that the volume fraction of SPNPs, and therefore the magnetizability of the microparticles, can be easily controlled by varying the volume percentage.

To illustrate this approach, $CoFe_2O_4$ SPNPs with oleic acid ligands were prepared by thermal decomposition.[46] Figure 1D shows a transmission electron microscopic image of the synthesized SPNPs. SQUID measurements of the magnetic hysteresis of the synthesized SPNPs clearly show superparamagnetic properties (Figure 3D), and X-ray diffraction measurements confirm a spinel structure for the $CoFe_2O_4$ SPNPs (Supporting information, Figure S2). By mixing a 4 wt% SPNP solution in toluene with the photoresist, the same photolithographic process was performed to synthesize 4 μm-side triangular particles (Figure 1B), eventually yielding 1 wt% solution of triangular paramagnetic microparticles in 1 mM of Tris-HCl buffer (pH = 8.3) for storage.

To make 2D suspensions of these paramagnetic micro particles at water/decane interfaces, a 5:3:2 ratio mixture of water, isopropanol, and microparticle solution was spread using a microsyringe. The microparticles naturally orient parallel to the liquid/liquid interface, with the SAM-coated (hydrophobic) side favoring contact with the decane. The Janus character of the microparticles, arising from the evaporatively-deposited gold layer, yields planar contact line that suppress capillary interactions between neighboring particles. This stands in marked contrast with chemically homogeneous particles (e.g., colloidal ellipsoids formed by film-stretching), which naturally exhibit

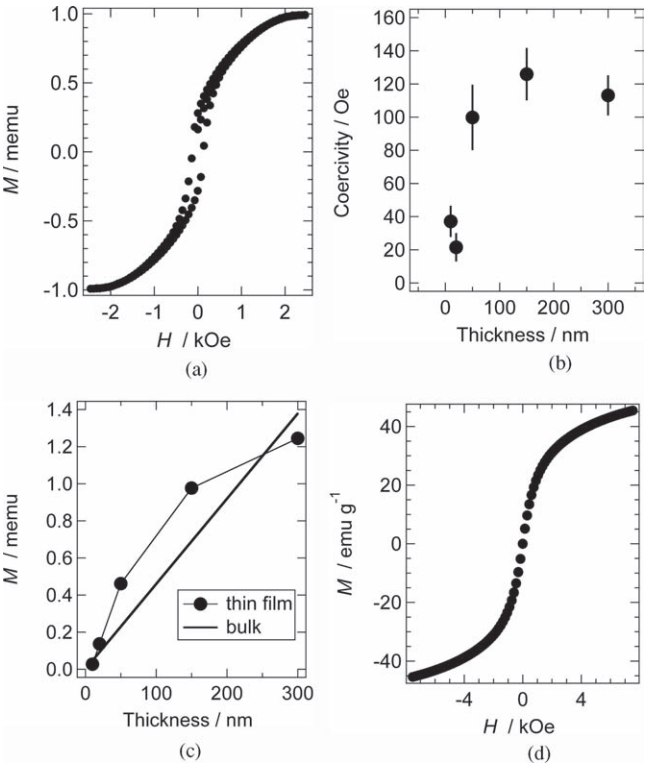

Figure 3. A) *M-H* curve for a batch of 20 μm-diameter microdisks with 150 nm Ni layers, fabricated following the procedure in Figure 1A. The ferromagnetic response is clearly evident: hysteresis, coercivity, and remnant magnetization. B) Coercivity of ferromagnetic microdisks as a function of evaporated Nickel film thickness. C) Saturation magnetization of nickel thin films as a function of thickness (circles), compared with and expectations based on equivalent volumes of bulk nickel (solid line). D) *M-H* curve for $CoFe_2O_4$ superparamagnetic nanoparticles shows strong saturation magnetization, but no hysteresis or coercivity.

non-planar contact lines that cause strong, long-ranged interactions and aggregation.[17,18] **Figure 4**A shows the random initial configuration of the microparticles at the water/decane interface after spreading. Applying a field parallel to the surface gives rise to anisotropic interactions between microparticles, with chaining along the field lines (generally point-to-point where the induced field gradients are strongest), and repulsion between microparticle chains (Figure 4B). Chains fragment and particles slowly disperse due to Brownian motion when the field is removed, establishing the reversibility of the field-induced aggregation (Supporting Information, Figure S3). Although paramagnetic microparticles in bulk water also form chains in response to an applied field, the orientation of each microparticle is randomly distributed due to the lack of an interface (Figure 4C).

We have demonstrated that a photolithographic process along with evaporative metal deposition offers an extremely versatile route to the synthesis of multifunctional microparticles possessing magnetic, amphiphilic, and anisotropic structural features. The ability to control various aspects of these structural features allows microfabricated ferromagnetic disks to be fabricated and used as exquisite probes of the rheological properties of complex fluid interfaces. The modularity of this design strategy also allows the corresponding paramagnetic microtriangles to be prepared for the analysis of 2D suspensions at fluid/fluid interfaces. Of course, the total yield is limited (here to 10^7–10^8 particles per 4" wafer) by the 2D surface nature of the fabrication, but could be scaled up, e.g., using imprint lithography techniques if needed. Nonetheless, these studies demonstrate the power of these fabrication techniques and the rich array of microstructures that can be easily prepared with control over size, aspect ratio, and shape via photolithography; magnetic properties by controlling the thickness of the deposited metal for ferromagnetic particles or the volume fraction of SPNPs for paramagnetic particles; and chemical anisotropy by selecting appropriate thiol-terminated molecules to self-assemble into monolayers on the gold surface.

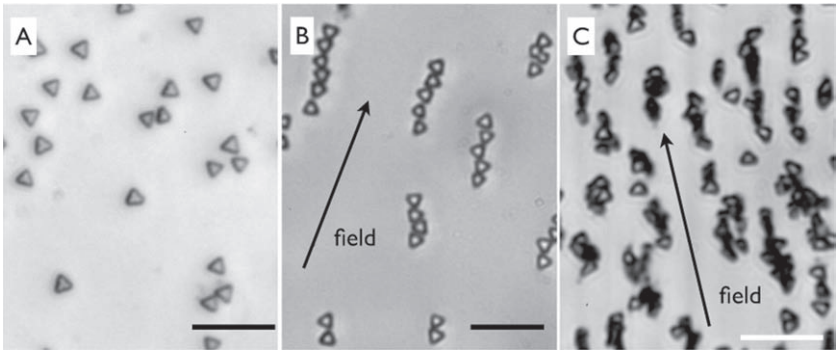

Figure 4. A) 4 μm paramagnetic, Janus triangles spread at a water/decane interface. Their configuration and orientation are random, and electrostatic stabilization prevents irreversible aggregation. Notably, the planar contact line prevents aggregation due to capillary interactions, as occurs with chemically homogeneous, anisotropically-shaped colloids.[17,41] B) A 10 mT magnetic field applied parallel to the interface causes the triangles to form chain-like structures along the field direction. The Janus (amphiphilic) nature of the two triangle faces keeps them oriented within the plane of the interface. C) Janus triangles submerged in bulk water also form chains under 10 mT fields, but each triangle of the chain orients randomly. Scale bar: 20 μm.

Supporting Information

Supporting Information is available from the Wiley Online Library or from the author.

Acknowledgements

The authors acknowledge primary support from the NSF MRSEC program (DMR-0520415) and additional support from the Beckman Young Investigator Program. A portion of this work was done in the UCSB nanofabrication facility, part of the NSF-funded NNIN network, and a portion performed in the MRL Central Facilities, supported by the MRSEC Program of the NSF under Award No. DMR05–20415; a member of the NSF-funded Materials Research Facilities Network. M. Kemei and R. Seshadri's help for the SQUID measurements is gratefully acknowledged. This article is part of the Special Issue on Materials Research at the University of California, Santa Barbara.

Received: October 2, 2010
Revised: January 7, 2011
Published online: March 1, 2011

[1] B. Lindlar, M. Boldt, S. Eiden-Assmann, G. Maret, *Adv. Mater.* **2002**, *14*, 1656.
[2] N. Pamme, *Lab Chip* **2006**, *6*, 24.
[3] J. Ge, Y. Hu, Y. Yin, *Angew. Chem. Int. Ed.* **2007**, *46*, 7428.
[4] J. Lee, Y. Jun, S. Yeon, J. Shin, J. Cheon, *Angew. Chem. Int. Ed.* **2006**, *45*, 8160.
[5] P. A. Voltairas, D. I. Fotiadis, L. K. Michalis, *J. Biomech.* **2002**, *35*, 813.
[6] J. Choi, K. W. Oh, J. H. Thomas, W. R. Heineman, H. B. Halsall, J. H. Nevin, A. J. Helmicki, H. T. Henderson, C. H. Ahn, *Lab Chip* **2002**, *2*, 27.
[7] O. A. Saleh, D. B. McIntosh, P. Pincus, N. Ribeck, *Phys. Rev. Lett.* **2009**, *102*, 068301.
[8] H. Kim, J. Ge, J. Kim, S. Choi, H. Lee, H. Lee, W. Park, Y. Yin, S. Kwon, *Nat. Photon.* **2009**, *3*, 534.
[9] F. Amblard, A. C. Maggs, B. Yurke, A. N. Pargellis, S. Leibler, *Phys. Rev. Lett.* **1996**, *77*, 4470.
[10] L. Deng, X. Trepat, J. P. Butler, E. Millet, K. G. Morgan, D. A. Weitz, J. J. Fredberg, *Nat. Mater.* **2006**, *5*, 636.
[11] B. D. Hoffman, G. Massiera, K. M. Van Citters, J. C. Crocker, *Proc. Natl. Acad. Sci. USA* **2006**, *103*, 10259.
[12] D. Zerrouki, J. Baudry, D. Pine, P. Chaikin, J. Bibette, *Nature* **2008**, *455*, 380.
[13] R. M. Erb, H. S. Son, B. Samanta, V. M. Rotello, B. B. Yellen, *Nature* **2009**, *457*, 999.
[14] H. Xia, J. Wang, Y. Tian, Q. Chen, X. Du, Y. Zhang, Y. He, H. Sun, *Adv. Mater.* **2010**, *22*, 3204.
[15] C. Guerrero-Sanchez, T. Lara-Ceniceros, E. Jimenez-Regalado, M. Ra a, U. Schubert, *Adv. Mater.* **2007**, *19*, 1740.
[16] J. A. Champion, Y. K. Katare, S. Mitragotri, *Proc. Natl. Acad. Sci. USA* **2007**, *104*, 11901.
[17] K. J. Stebe, E. Lewandowski, M. Ghosh, *Science* **2009**, *325*, 159.
[18] B. Madivala, J. Fransaer, J. Vermant, *Langmuir* **2009**, *25*, 2718.
[19] C. P. Lapointe, T. G. Mason, I. I. Smalyukh, *Science* **2009**, *326*, 1083.
[20] M. J. Solomon, P. T. Spicer, *Soft Matter* **2010**, *6*, 1391.
[21] S. C. Glotzer, M. J. Solomon, *Nat Mater* **2007**, *6*, 557.
[22] K. Zhao, T. G. Mason, *Phys. Rev. Lett.* **2009**, *103*, 208302.
[23] R. C. Kramb, R. Zhang, K. S. Schweizer, C. F. Zukoski, *Phys. Rev. Lett.* **2010**, *105*, 055702.
[24] J. C. Loudet, A. G. Yodh, B. Pouligny, *Phys. Rev. Lett.* **2006**, *97*, 018304.
[25] J. P. Rolland, B. W. Maynor, L. E. Euliss, A. E. Exner, G. M. Denison, J. M. DeSimone, *J. Am. Chem. Soc.* **2005**, *127*, 10096.
[26] S. Kim, S. Lee, S. Yang, *Angew. Chem. Int. Ed.* **2010**, *49*, 2535.
[27] K. Roh, D. C. Martin, J. Lahann, *Nat. Mater.* **2005**, *4*, 759.
[28] S. Jiang, Q. Chen, M. Tripathy, E. Luijten, K. S. Schweizer, S. Granick, *Adv. Mater.* **2010**, *22*, 1060.
[29] F. Wurm, A. F. M. Kilbinger, *Angew. Chem. Int. Ed.* **2009**, *48*, 8412.
[30] A. Walther, A. Müller, *Soft Matter* **2008**, *4*, 663.
[31] S. Granick, S. Jiang, Q. Chen, *Phys. Today* **2009**, *62*, 68.
[32] S. Q. Choi, S. Steltenkamp, J. A. Zasadzinski, T. M. Squires, unpublished.
[33] S. Badaire, C. Cottin-Bizonne, J. W. Woody, A. Yang, A. D. Stroock, *J. Am. Chem. Soc.* **2007**, *129*, 40.
[34] J. Moon, A. Kim, J. Crocker, S. Yang, *Adv. Mater.* **2007**, *19*, 2508.
[35] C. Hernandez, T. Mason, *J. Phys. Chem. C* **2007**, *111*, 4477.
[36] K. Masschaele, B. J. Park, E. M. Furst, J. Fransaer, J. Vermant, *Phys. Rev. Lett.* **2010**, *105*, 048303.
[37] D. C. Jiles, T. T. Chang, D. R. Hougen, R. Ranjan, *J. Appl. Phys.* **1988**, *64*, 3620.
[38] B. P. Binks, *Curr. Opin. Colloid Interface Sci.* **2002**, *7*, 21.
[39] A. B. Subramaniam, M. Abkarian, H. A. Stone, *Nat Mater* **2005**, *4*, 553.
[40] E. M. Herzig, K. A. White, A. B. Schofield, W. C. K. Poon, P. S. Clegg, *Nat. Mater.* **2007**, *6*, 966.
[41] K. Masschaele, J. Vermant, J. Fransaer, *J. Rheol.* **2009**, *53*, 1437.
[42] D. Klingenberg, *AIChE Journal* **2001**, *47*, 246.
[43] S. Kim, J. Sim, J. Lim, S. Yang, *Angew. Chem. Int. Ed.* **2010**, *49*, 3786.
[44] S. N. Ahmad, S. G. Rao, S. A. Shaheen, D. Magana, G. F. Strouse, *Appl. Phys. Lett.* **2008**, *92*, 112511.
[45] D. K. Hwang, D. Dendukuri, P. S. Doyle, *Lab Chip* **2008**, *8*, 1640.
[46] S. Sun, H. Zeng, D. B. Robinson, S. Raoux, P. M. Rice, S. X. Wang, G. Li, *J. Am. Chem. Soc.* **2004**, *126*, 273.